THE JOURNAL OF
PHYSICAL CHEMISTRY B

Photoelectron Spectroscopy of BiAu$^-$ and BiBO$^-$: Further Evidence of the Analogy between Au and Boronyl

Tian Jian, Gary V. Lopez, and Lai-Sheng Wang*

Department of Chemistry, Brown University, Providence, Rhode Island 02912, United States

ABSTRACT: Boronyl (BO) is a monovalent σ radical with a B≡O triple bond. Its chemistry has remained relatively unknown, though analogy has been established for BO with monovalent atoms, such as H or Au. Here we report a photoelectron spectroscopic study of BiAu$^-$ and BiBO$^-$, showing further evidence of the analogy between Au and BO. The photoelectron spectra of BiAu$^-$ and BiBO$^-$ are found to be similar, suggesting that they possess similar electronic structure and chemical bonding. The electron affinities of BiAu and BiBO are measured to be 1.38(4) and 1.84(3) eV, respectively. The ground states of both BiAu and BiBO are shown to be a triplet (X $^3\Sigma^-$). In addition, vibrational structures are resolved in the spectra of BiBO$^-$. Two vibrational frequencies at 320(30) and 1860(50) cm^{-1} are measured for the ground state of BiBO, corresponding to the Bi−B and B−O stretching modes, respectively. The low-lying electronic excited states of BiAu and BiBO are also found to be similar: their first four excited states are A $^1\Delta$, B $^1\Sigma^+$, C $^3\Pi$, and D $^1\Pi$, with excitation energies at 0.71, 1.29, 2.54, and 2.67 eV for BiAu and 0.63, 1.26, 3.68, and 3.82 eV for BiBO, respectively, above the $^3\Sigma^-$ ground state. Weak photoelectron features related to two-electron detachment transitions are also observed for both anions because of strong electron correlation effects in the ground state of the anions.

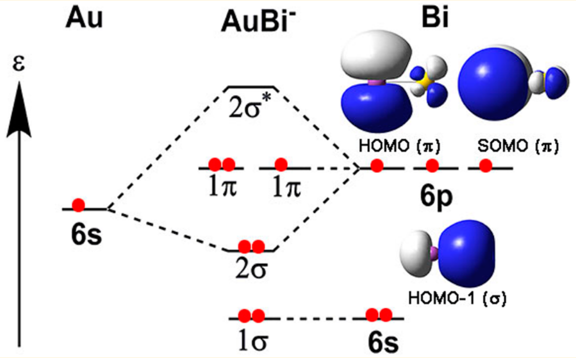

1. INTRODUCTION

Bismuth has been of interest recently because of its importance in topological-insulators,[1] which are a new class of solid materials with extrordnary electronic properties. Investigations of finite systems contianing Bi can yield valuable information about its bonding properties. The electronic structures of both neutral and anionic Bi clusters have been investigated by photoelectron spectroscopy (PES).[2−10] PES has also been applied to anions of gaseous Bi complexes[11−13] and bimetallic Bi clusters.[14−20] There have been theoretical investigations about the electronic and structural properties of neutral and anionic Bi clusters,[21−26] as well as binary Bi clusters.[27−32] The structures of cationic bismuth clusters have been probed experimentally by ion mobility and trapped ion electron diffraction.[33] In the current article, we report a PES study of two Bi-containing molecular species, a diatomic BiAu$^-$ and a BiBO$^-$ complex, to examine the bonding properties of Bi with Au and boronyl.

The structural and bonding properties of boron are fascinating in chemistry and have attracted significant recent attention.[34] The chemistry of boron exhibits a vast structural diversity, featuring icosahedral B_{12} or other polyhedral cages as key structural units.[35] Even though the electron deficiency of boron often gives rise to multicenter bonding via electron delocalization in the polyhedral cages in bulk boron and, in particular, in planar boron clusters,[36] boron can also form strong multiple covalent bonds. For example, PES and theoretical studies have shown that boronyl (BO), which is isoelectronic with CN, has a strong triple bond.[34,37−39] The closed-shell BO$^-$ anion is isoelectronic with CN$^-$ and CO, while the boronyl BO is a monovlaent σ radical. The chemistry of boronyl is relatively unknown. Prior PES and theoretical studies have shown that $Au_n(BO)^-$ (n = 1−3), $B_{10}BO^-$, $B_{12}BO^-$, and $B_3(BO)_n^-$ (n = 1, 2) possess bonding and structures similar to Au_{n+1}^- (n = 1−3), $B_{10}Au^-$, $B_{12}Au^-$, and $B_3Au_n^-$ (n = 1, 2), respectively, establishing the analogy between BO and Au.[40−43] Recently, the first platinum BO compound has been synthesized and isolated,[44] further demonstrating the structural robustness of the boronyl group. Hence, many new boronyl compounds may exist, analogous to that of CN or CO.[34]

Here we report a PES study of BiAu$^-$ and BiBO$^-$ to extend the Au and BO analogy in their bonding to Bi. Photoelectron spectra of BiAu$^-$ and BiBO$^-$ are observed to be similar, indicating their similar electronic structure and bonding. It is found that the BO unit behaves as a monodentate ligand to bismuth and mimics the gold atom to give a linear BiBO structure. The electron affinities of BiAu and BiBO are measured to be 1.38(4) and 1.84(3) eV, respectively. The first four low-lying electronic excited states of the two species are also reported.

2. EXPERIMENTAL METHODS

The experiment was carried out using a magnetic-bottle PES apparatus equipped with a laser vaporization supersonic cluster source, details of which have been described elsewhere.[45] Briefly,

Special Issue: Bruce C. Garrett Festschrift

Received: August 26, 2015
Published: October 5, 2015

DOI: 10.1021/acs.jpcb.5b08327
J. Phys. Chem. B 2016, 120, 1635−1640

the $BiAu^-$ and $BiBO^-$ anions were produced by laser vaporization of a Bi/^{11}B/Au mixed target with a helium carrier gas seeded with 5% argon. The oxygen impurity that led to the formation of $BiBO^-$ was most likely from the target, which was cold-pressed from a mixture of Au, isotopically enriched ^{11}B, and Bi powders. Both pure boron clusters and a variety of mixed clusters were produced. The $BiAu^-$ and $BiBO^-$ anions of interest were each mass-selected and decelerated before being photodetached by a pulsed laser beam. Photoelectrons were collected at nearly 100% efficiency by a magnetic bottle and analyzed in a 3.5 m long electron flight tube. The photodetachment experiment was conducted at four detachment photon energies: 532 nm (2.331 eV), 355 nm (3.496 eV), and 266 nm (4.661 eV) from a Nd:YAG laser and 193 nm (6.424 eV) from an ArF excimer laser. Photoelectron spectra were calibrated by using the known spectra of Au^- and Bi^-, and the energy resolution of the apparatus was $\Delta E_k/E_k \approx 2.5\%$, that is, approximately 25 meV for 1 eV electrons.

3. RESULTS

The photoelectron spectra are shown in Figure 1 for $BiAu^-$ and Figure 2 for $BiBO^-$. The observed binding energies for all peaks, their assignments, and the obtained spectroscopic information are summarized in Tables 1 and 2 for $BiAu^-$ and $BiBO^-$, respectively.

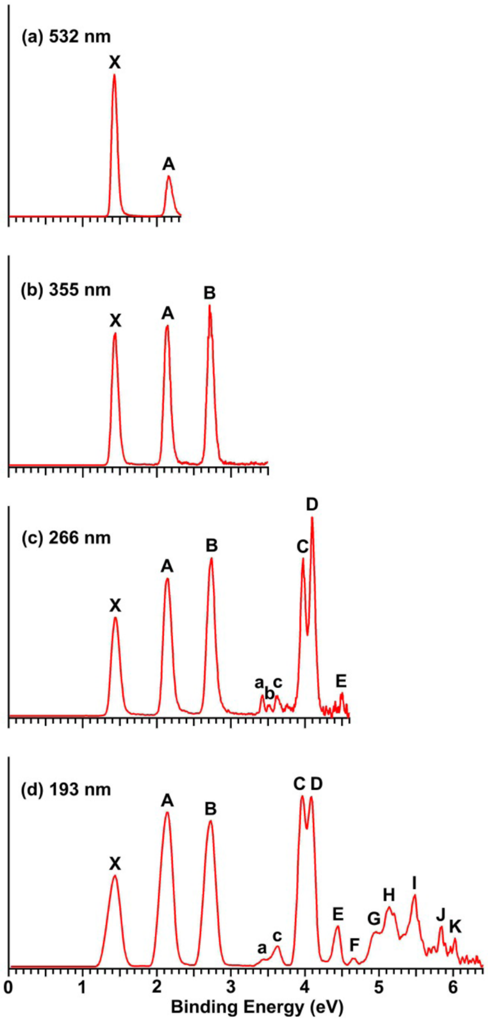

Figure 1. Photoelectron spectra of $BiAu^-$ at four detachment photon energies: (a) 532 nm, (b) 355 nm, (c) 266 nm, and (d) 193 nm.

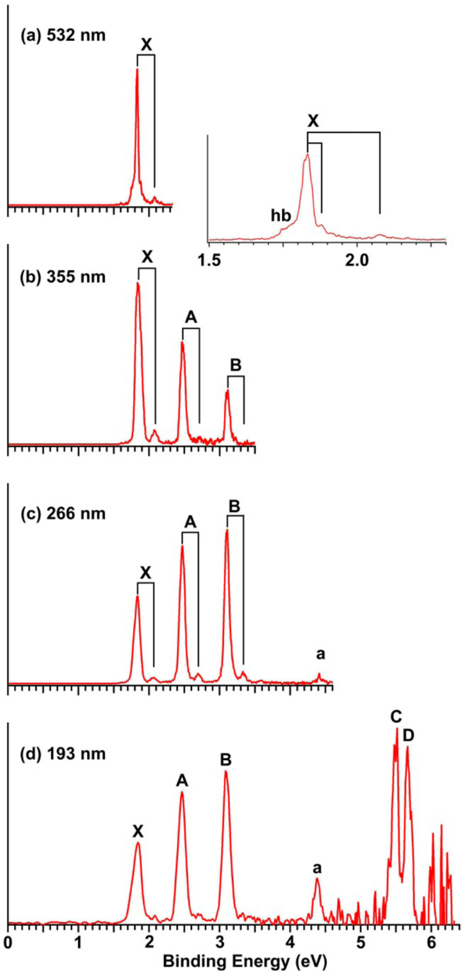

Figure 2. Photoelectron spectra of $BiBO^-$ at four detachment photon energies: (a) 532 nm, (b) 355 nm, (c) 266 nm, and (d) 193 nm. The inset shows an expanded view of the 532 nm spectrum. "hb" stands for hot band. The vertical lines indicate vibrational structures.

3.1. $BiAu^-$. The 532 nm spectrum of $BiAu^-$ (Figure 1a) displays two sharp peaks. The ground-state peak X is observed at a vertical detachment energy (VDE) of 1.43 eV. Because no vibrational structures were resolved, the adiabatic detachment energy (ADE) of this peak was estimated by drawing a straight line along its rising edge and then adding the instrumental resolution to the intersection with the binding energy axis. The ADE so determined is 1.38 ± 0.04 eV, which also represents the electron affinity (EA) of neutral BiAu. The difference between the ADE and VDE indicates that the X band is likely composed of an unresolved vibrational progression, suggesting that there is probably a small geometry change between the anion ground state and that of the neutral. Another feature labeled as A at a VDE of 2.14 eV is relatively weak, and its intensity seems to increase with photon energies. The spectrum at 355 nm (Figure 1b) shows one more sharp and intense peak (B) at 2.72 eV. The spectrum at 266 nm (Figure 1c) exhibits two more intense and closely spaced peaks, C (VDE: 3.97 eV) and D (VDE: 4.10 eV), following a large energy gap of ~1.3 eV from the B band. A number of weak peaks (a, b, c) are observed in the energy gap. A weak peak (E) is also observed at 4.44 eV in the 266 nm spectrum, and its intensity increases slightly at 193 nm (Figure

Table 1. Observed Vertical Detachment Energies (VDEs) of $BiAu^-$ and Their Assignments, and the Obtained Electron Affinity (EA) and Term Values for BiAu[a]

observed features and assignment	VDE (eV)	EA (eV)	term value (eV)
X $^3\Sigma^-$ ($1\sigma^2 2\sigma^2 1\pi^2$)	1.43(4)	1.38(4)	0
A $^1\Delta$ ($1\sigma^2 2\sigma^2 1\pi^2$)	2.14(4)		0.71(4)
B $^1\Sigma^-$ ($1\sigma^2 2\sigma^2 1\pi^2$)	2.72(2)		1.29(4)
C $^3\Pi$ ($1\sigma^2 2\sigma^1 1\pi^3$)	3.97(2)		2.54(4)
D $^1\Pi$ ($1\sigma^2 2\sigma^1 1\pi^3$)	4.10(2)		2.67(4)
E	4.44(5)		3.01(5)
F	4.65(5)		3.22(5)
G	4.94(5)		3.51(5)
H	5.14(5)		3.71(5)
I	5.48(5)		4.05(5)
J	5.84(5)		4.41(5)
K	6.02(5)		4.59(5)
a	3.42(3)[b]		1.99(4)
b	3.52(3)[b]		2.09(4)
c	3.62(3)[b]		2.19(4)

[a] Numbers in the parentheses represent experimental uncertainties in the last digit. [b] These features are likely due to two-electron processes.

Table 2. Observed Vertical Detachment Energies (VDEs) of $BiBO^-$ and Their Assignments, and the Obtained Electron Affinity (EA), Term Values, and Vibrational Frequencies for BiBO[a]

observed features and assignment	VDE (eV)	EA (eV)	term value (eV)	vib. freq (cm^{-1})
X $^3\Sigma^-$ ($1\sigma^2 2\sigma^2 1\pi^2$)	1.84(3)	1.84(3)	0	320(30),[c] 1860(50)[d]
A $^1\Delta$ ($1\sigma^2 2\sigma^2 1\pi^2$)	2.47(3)		0.63(3)	1860(50)[d]
B $^1\Sigma^-$ ($1\sigma^2 2\sigma^2 1\pi^2$)	3.10(3)		1.26(3)	1860(50)[d]
C $^3\Pi$ ($1\sigma^2 2\sigma^1 1\pi^3$)	5.52(5)		3.68(5)	
D $^1\Pi$ ($1\sigma^2 2\sigma^1 1\pi^3$)	5.66(5)		3.82(5)	
a	4.38(5)[b]		2.54(5)	

[a] Numbers in the parentheses represent experimental uncertainties in the last digit. [b] This feature is likely due to a two-electron process. [c] For the Bi−B stretching mode. [d] For the B−O stretching mode.

1d). Beyond peak E, the spectrum at 193 nm becomes congested with numerous relatively weak peaks (F−K), which are probably due to detachment of the Au 5d electrons.

3.2. $BiBO^-$. The overall spectral pattern of $BiBO^-$ (Figure 2) is very similar to that of $BiAu^-$, in terms of the five major bands (X, A−D), except in the case of $BiBO^-$ vibrational features are also observed for bands X, A, and B. At 532 nm (Figure 2a), a sharp peak is observed with two short vibrational progressions for the ground-state detachment transition (X) with frequencies of 320 and 1860 cm^{-1} (see insert). The 0−0 transition defines the EA for the BiBO neutral molecule as 1.84 eV, which also represents the ground-state VDE of the anion. Hot band transitions (hb) are also observed, as shown in the inset of Figure 2. The weak vibrational features of band X suggest little geometry change between the anion ground state and that of neutral BiBO. At 355 and 266 nm, two more intense peaks are observed, A at 2.47 eV and B at 3.10 eV, each with a short vibrational progression of 1860 cm^{-1}. The 266 nm spectrum (Figure 2c) also shows a weak peak (labeled as a) at 4.38 eV. The intensity of this peak increases at 193 nm (Figure 2d), where two closely spaced intense peaks C and D are observed at 5.52 and 5.66 eV, respectively, following a large energy gap of 2.4 eV from band B. The spikes beyond 6 eV are due to noise because of the poor signal-to-noise ratio in this part of the spectrum.

4. DISCUSSION

4.1. General Bonding Considerations. The similarity between the main photoelectron spectral features of $BiAu^-$ and $BiBO^-$ suggests that the two anions possess similar bonding and electronic structure. We will use $BiAu^-$ as an example for some general consideration of the bonding in these two species. The valence electron configuration of Bi is $6s^2 6p^3$. However, because of the strong relativistic effects,[46] the 6s orbital is significantly stabilized and is unlikely to participate in bonding with Au. Hence, only the 6p orbital is expected to bond with the Au 6s orbital to form a σ bond in BiAu. The $6p_z$ orbital of Bi is expected to form the σ bond with the Au 6s orbital, whereas the $6p_x$ and $6p_y$ orbitals are expected to form a nonbonding π orbital. The valence electron configuration of $BiAu^-$ from this simple consideration can be represented by the schematic molecular orbital (MO) diagram depicted in Figure 3. Thus, the ground-state valence electron configuration of $BiAu^-$ is $1\sigma^2 2\sigma^2 1\pi^3$, resulting in a $^2\Pi$ electronic ground state. The $BiBO^-$ anion is expected to have a similar electronic structure, where the BO unit contributes an sp electron to form a σ bond with the $6p_z$ orbital of Bi.

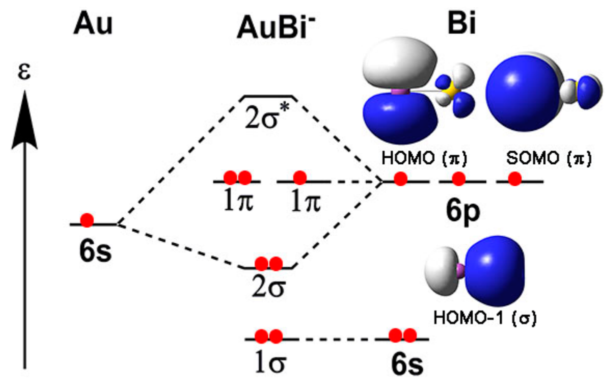

Figure 3. Schematic orbital diagram for $BiAu^-$, showing the bonding interactions between the Au 6s and Bi 6p orbitals.

Figure 4 shows the structures and MO pictures for $BiAu^-$ and $BiBO^-$. The MOs were obtained by single-point calculation using PW91/Bi,Au/Stuttgart level of theory in Gaussian 09[47] and plotted with GaussView.[48] In the case of $BiAu^-$ (Figure 4a), the singly occupied molecular orbital (SOMO) and highest occupied molecular orbital (HOMO) are degenerate π orbitals mainly consisting of Bi $6p_{x,y}$ atomic orbitals with slightly antibonding contributions from the Au 5d atomic orbitals. The HOMO−1 molecular orbital is formed by the overlap of the Au 6s orbital and the Bi $6p_z$ orbital, which is responsible for the σ bond between Bi and Au. The MOs from HOMO−2 to HOMO−6 are mainly related to the Au 5d orbitals. The HOMO−7 is primarily the Bi 6s orbital. The SOMO and HOMO of $BiBO^-$ (Figure 4b) are similar to those of $BiAu^-$, whereas the HOMO−5 (Bi 6s) of $BiBO^-$ is the same as HOMO−7 in $BiAu^-$. The remaining MOs of $BiBO^-$ come from the boronyl unit. The HOMO−2, HOMO−3, and HOMO−4 represent the triple bond of B≡O, while the HOMO−6 is primarily from the O 2s orbital.

The main PES features of $BiAu^-$ and $BiBO^-$ can be readily assigned using the MO pictures discussed above, as given in detail in Tables 1 and 2, respectively.

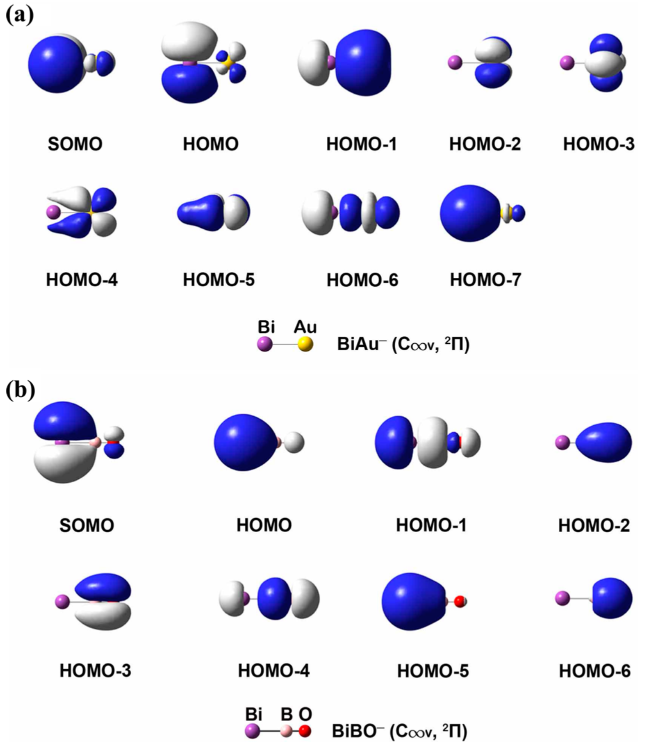

Figure 4. Molecular orbital pictures for (a) $BiAu^-$ and (b) $BiBO^-$.

4.2. $BiAu^-$. As shown in Figures 3 and 4, the ground state of $BiAu^-$ is a double state ($^2\Pi$) with a $1\sigma^2 2\sigma^2 1\pi^3$ valence configuration. One-electron detachment from the 1π and 2σ MOs can result in five final states:

$$1\sigma^2 2\sigma^2 1\pi^3(^2\Pi) \rightarrow 1\sigma^2 2\sigma^2 1\pi^2, \quad {}^3\Sigma^-, {}^1\Delta, {}^1\Sigma^+ \tag{1}$$

$$\rightarrow 1\sigma^2 2\sigma^1 1\pi^3, \quad {}^3\Pi, {}^1\Pi \tag{2}$$

These five final states are indeed borne out from the observed photoelectron spectra in Figure 1, corresponding to the five main PES features, X and A–D. The removal of one electron from the 1π orbital results in three final states, $^3\Sigma^-$, $^1\Delta$, and $^1\Sigma^+$. According to Hund's rules, the $^3\Sigma^-$ state is the ground state, corresponding to the X band. The $^1\Delta$ state is the first excited state, corresponding to the A band, whereas the $^1\Sigma^+$ state is assigned to the B band. The shape and relative intensities of the X, A, and B bands are similar, consistent with their common electron configuration. One-electron detachment from the HOMO−1 orbital (2σ) results in the $^3\Pi$ and $^1\Pi$ final states, which should correspond to bands C and D, respectively. Figure 5 shows schematically the energy levels of these five electronic states of the BiAu dimer and their measured excitation energies.

The weak features, a–c, fall in the gap between the 1π and 2σ MOs and cannot be due to one-electron transitions. They are likely derived from two-electron processes, i.e., detachment of a 1π electron while simultaneously exciting a 1π electron to the $2\sigma^*$ orbital (Figure 3), resulting in a $1\sigma^2 2\sigma^2 1\pi^1 2\sigma^{*1}$ final configuration. Such two-electron transitions or so-called shakeup processes[49] are direct reflections of the electron correlation effects in the ground state of $BiAu^-$. The congested signals at higher binding energies beyond band D (Figure 1d) should be mainly due to detachment from the five Au 5d-based MOs (Figure 4a), resulting in a high density of final states, as a result of spin–spin and spin–orbit couplings. This part of the spectrum may also contain two-electron transitions.

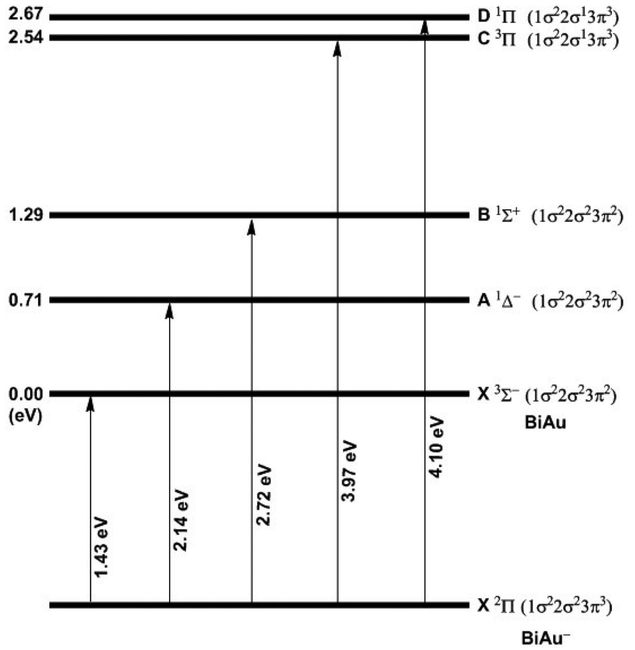

Figure 5. Photodetachment transitions from the $BiAu^-$ ground state to the ground state and four excited states of BiAu. The measured electron binding energies for the detachment transitions and the excitation energies of the four low-lying electronic excited states of BiAu are given (see Table 1).

4.3. $BiBO^-$. The photoelectron spectra of $BiBO^-$ can be understood straightforwardly, following the discussion of the $BiAu^-$ spectra, because of their similarity. $BiBO^-$ should have a linear structure ($C_{\infty v}$) with a doublet ground state ($^2\Pi$) and a valence electron configuration of $1\sigma^2 2\sigma^2 1\pi^3$, similar to $BiAu^-$ (Figure 3). The removal of one electron from the 1π orbital results in three final states, $^3\Sigma^-$, $^1\Delta$, and $^1\Sigma^+$, corresponding to the X, A, and B bands, respectively. Two vibrational frequencies were resolved for the $^3\Sigma^-$ ground state (320 and 1860 cm^{-1}), which should be due to the Bi–B and B–O stretching, respectively. For comparison, we calculated the frequencies of the optimized linear structure of BiBO using the PW91/Bi/Stugart/B,O/Aug-ccpVTZ level of theory in Gaussian 09. The calculated frequencies for the Bi–B and B–O stretching modes were 354 and 1815 cm^{-1}, respectively, in good agreement with the experimental observation. A vibrational feature was observed in bands A and B with a frequency of 1860 cm^{-1}, which should also be due to the B–O stretching mode. The same B–O vibrational frequency (1860 cm^{-1}) observed for bands X, A, and B is consistent with the fact that they all derive from the same electron configuration. We note that the B–O stretching vibrational frequency in BiBO is very similar to that in the free BO unit.[38,39]

Detachment from the HOMO−1 (2σ) produces the $^3\Pi$ and $^1\Pi$ final states, corresponding to bands C and D, respectively, similar to the case of $BiAu^-$. A weak feature (a) was also observed between bands B and C, which should be related to a two-electron transition, as discussed above for the case of $BiAu^-$. Different from $BiAu^-$, there were no major PES signals observed beyond band D because of the expected high binding energies of the three MOs responsible for the B≡O triple bond (Figure 4b). The electron binding energy of the π MO in bare BO^- was observed previously to be around 5.5 eV with a broad Franck–Condon envelope.[38] The binding energy of the same π MO in

BiBO is expected to be much higher. An energy level diagram similar to Figure 5 can also be made for BiBO. The excitation energies of the observed energy levels are given in Table 2.

5. CONCLUSIONS

We have produced two Bi-containing species, $BiAu^-$ and $BiBO^-$, and investigated their electronic structures using photoelectron spectroscopy. Well-resolved photoelectron spectra are obtained for the two anions at various photon energies, and the electron affinities and low-lying electronic excited states of the neutral BiAu and BiBO molecules are reported. The photoelectron spectra of the two species are similar, providing spectroscopic evidence for the analogy between Au and BO in their bonding to a main group element. The electron affinities of BiAu and BiBO are measured to be 1.38(4) and 1.84(3) eV, respectively. Both BiAu and BiBO are found to have the same ground electronic states ($X\ ^3\Sigma^-$). Four low-lying excited states for each species are observed, and their excitation energies are reported. Two-electron transitions are observed in the photoelectron spectra of both anions, indicating strong electron correlation effects in their ground states.

■ AUTHOR INFORMATION

Corresponding Author

*E-mail: lai-sheng_wang@brown.edu.

Notes

The authors declare no competing financial interest.

■ ACKNOWLEDGMENTS

This work was supported by the National Science Foundation (Grant CHE-1263745).

■ REFERENCES

(1) Zhang, H. J.; Liu, C. X.; Qi, X. L.; Dai, X.; Fang, Z.; Zhang, S. C. Topological Insulators in Bi_2Se_3, Bi_2Te_3 and Sb_2Te_3 with a Single Dirac Cone on the Surface. *Nat. Phys.* **2009**, *5*, 438−442.

(2) Suzer, S.; Lee, S. T.; Shirley, D. A. PES of Atomic and Molecular Bismuth. *J. Chem. Phys.* **1976**, *65*, 412−417.

(3) Kajita, A.; Saito, Y.; Yasue, T.; Hayashi, M.; Ichimiya, A.; Gotoh, T.; Kawaguchi, Y.; Kotani, M.; Shigeta, Y.; Takagi, S.; Tazawa, Y.; Ohtani, S. Threshold Behavior of Synchrotron Radiation Photoionization for Bi_n ($n \leq 4$). *J. Phys. Soc. Jpn.* **1989**, *58*, 2320−2324.

(4) Wang, L. S.; Lee, Y. T.; Shirley, D. A.; Balasubramanian, K.; Feng, P. Photoelectron Spectroscopy and Electronic Structure of Clusters of the Group V Elements. I. Dimers. *J. Chem. Phys.* **1990**, *93*, 6310−6317.

(5) Saito, Y.; Kajita, A.; Yasue, T.; Hayashi, M.; Ichimiya, A.; Gotoh, T.; Kawaguchi, Y.; Kotani, M.; Shigeta, Y.; Takagi, S.; Tazawa, Y.; Ohtani, S. Photoionization Efficiency Curves in the Threshold Region for Bi_n ($n \leq 4$) Molecules. *Phys. Scr.* **1990**, *41*, 51−54.

(6) Polak, M. L.; Ho, J.; Gerber, G.; Lineberger, W. C. Photoelectron Spectroscopy of Negatively Charged Bismuth Clusters: Bi_2^-, Bi_3^- and Bi_4^-. *J. Chem. Phys.* **1991**, *95*, 3053−3063.

(7) Gausa, M.; Kaschner, R.; Seifert, G.; Faehrmann, J. H.; Lutz, H. O.; Meiwes-Broer, K. H. Photoelectron Investigations and Density Functional Calculations of Anionic Sb_n^- and Bi_n^- Clusters. *J. Chem. Phys.* **1996**, *104*, 9719−9728.

(8) Bowering, N.; Martins, M.; Snell, G.; Kuntze, R.; Heinzmann, U. Spin-Resolved Photoelectron Spectroscopy in the Autoionization Region of Atomic Bismuth. *J. Phys. B: At., Mol. Opt. Phys.* **1998**, *31*, 5221−5232.

(9) Zhai, H. J.; Wang, L. S.; Kuznetsov, A. E.; Boldyrev, A. I. Probing the Electronic Structure and Aromaticity of Pentapnictogen Cluster Anions Pn_5^- (Pn = P, As, Sb, and Bi) Using Photoelectron Spectroscopy and Ab Initio Calculations. *J. Phys. Chem. A* **2002**, *106*, 5600−5606.

(10) Mikkelä, M. H.; Tchaplyguine, M.; Urpelainen, S.; Jänkälä, K.; Björneholm, O.; Huttula, M. Photoelectron Spectroscopy of Unsupported Bismuth Clusters: Size Related Effects of Metallic Properties. *J. Appl. Phys.* **2012**, *112*, 084326.

(11) Sun, Z.; Sun, S.; Liu, H. T.; Zhu, Q.; Gao, Z.; Tang, Z. Photoelectron Spectroscopic and Theoretical Studies of $M_mC_6F_5$ Anionic Complexes (M = Pb and Bi; m = 1−4). *J. Phys. Chem. A* **2009**, *113*, 8045−8054.

(12) Sobhy, M. A.; Casalenuovo, K.; Reveles, J. U.; Gupta, U.; Khanna, S. N.; Castleman, A. W. Photoelectron Imaging and Density-Functional Investigation of Bismuth and Lead Anions Solvated in Ammonia Clusters. *J. Phys. Chem. A* **2010**, *114*, 11353−11363.

(13) Sun, Z.; Sun, S.; Liu, H. T.; Tang, Z.; Gao, Z. Photoelectron Spectroscopic and Theoretical Study of Aromatic−Bi_m Anionic Complexes (Aromatic = C_6H_5, C_5H_4N, C_4H_3O, and C_4H_4N; m = 1−3): A Comparative Study. *J. Phys. Chem. A* **2013**, *117*, 4127−4135.

(14) Sun, S.; Liu, H. T.; Tang, Z. Experimental and Theoretical Investigation on Binary Semiconductor Clusters of Bi/Si, Bi/Ge, and Bi/Sn. *J. Phys. Chem. A* **2006**, *110*, 5004−5009.

(15) Gupta, U.; Reber, A. C.; Clayborne, P. A.; Melko, J. J.; Khanna, S. N.; Castleman, A. W. Effect of Charge and Composition on the Structural Fluxionality and Stability of Nine Atom Tin-Bismuth Zintl Analogues. *Inorg. Chem.* **2008**, *47*, 10953−10958.

(16) Sobhy, M. A.; Reveles, J. U.; Gupta, U.; Khanna, S. N.; Castleman, A. W. Photoelectron Imaging and Theoretical Investigation of Bimetallic $Bi_{1-2}Ga_{0-2}^-$ and Pb_{1-4}^- Cluster Anions. *J. Chem. Phys.* **2009**, *130*, 054304.

(17) Gupta, U.; Reveles, J. U.; Melko, J. J.; Khanna, S. N.; Castleman, A. W. Origins of Stability in Mixed Bismuth-Indium Clusters. *J. Phys. Chem. C* **2010**, *114*, 15963−15972.

(18) Clayborne, P. A.; Gupta, U.; Reber, A. C.; Melko, J. J.; Khanna, S. N.; Castleman, A. W. The Applicability of Three-Dimensional Aromaticity in $BiSn_n^-$ Zintl Analogues. *J. Chem. Phys.* **2010**, *133*, 134302.

(19) Melko, J. J.; Werner, U.; Mitrić, R.; Bonačić-Koutecký, V.; Castleman, A. W. Electronic Structure Similarities in $Pb_xSb_y^-$ and $Sn_xBi_y^-$ Clusters. *J. Phys. Chem. A* **2011**, *115*, 10276−10280.

(20) Sun, Z.; Xu, H. G.; Feng, G.; Xu, X. L.; Zheng, W. J. Photoelectron Spectroscopy and Density Functional Theory Study of $Bi_2Al_n^-$ (n = 1−4) Clusters. *Chem. Phys. Lett.* **2014**, *615*, 56−61.

(21) Balasubramanian, K.; Sumathi, K.; Dai, D. Group V Trimers and Their Positive Ions: The Electronic Structure and Potential Energy Surfaces. *J. Chem. Phys.* **1991**, *95*, 3494−3505.

(22) Balasubramanian, K.; Liao, D. W. Spectroscopic Constants and Potential Energy Curves of Bi_2 and Bi_2^-. *J. Chem. Phys.* **1991**, *95*, 3064−3073.

(23) Choi, H.; Park, C.; Baeck, K. K. Ab Initio Study of the Geometries and Vibrational Properties of the Low-Lying Electronic States of Neutral and Anionic M_3 (M = P, As, Sb, and Bi): The Photoelectron Spectroscopy of the Anions. *J. Phys. Chem. A* **2002**, *106*, 5177−5187.

(24) Gao, L.; Li, P.; Lu, H.; Li, S. F.; Guo, Z. X. Size- and Charge-Dependent Geometric and Electronic Structures of Bi_n (Bi_n^-) Clusters, (n = 2−13) by First-Principles Simulations. *J. Chem. Phys.* **2008**, *128*, 194304.

(25) Jia, J. M.; Chen, G. B.; Shi, D. N.; Wang, B. L. Structural and Electronic Properties of Bi_n (n = 2−14) Clusters from Density-Functional Calculations. *Eur. Phys. J. D* **2008**, *47*, 359−365.

(26) Yuan, H. K.; Chen, H.; Kuang, A. L.; Miao, Y.; Xiong, Z. H. Density-Functional Study of Small Neutral and Cationic Bismuth Clusters Bi_n and Bi_n^+ (n = 2−24). *J. Chem. Phys.* **2008**, *128*, 094305.

(27) Chen, H.; Yuan, H. K.; Kuang, A. L.; Miao, Y.; Chen, P.; Xiong, Z. H. Geometrical Evolution, Electronic Structures, and Magnetic Properties of Bi-Mn Binary Clusters. *Phys. Rev. B: Condens. Matter Mater. Phys.* **2008**, *77*, 184429.

(28) Li, Z.; Zhao, C.; Chen, L. Structure and Aromaticity of Bi_5^-, Bi_5M (M = Li, Na, K) and Bi_5M^+ (M = Be, Mg, Ca) clusters. *J. Mol. Struct.: THEOCHEM* **2008**, *854*, 46−53.

DOI: 10.1021/acs.jpcb.5b08327
J. Phys. Chem. B 2016, 120, 1635−1640

(29) Sun, Z.; Zhu, Q.; Gao, Z.; Tang, Z. Experimental and Theoretical Investigation on Binary Anionic Clusters of $Al_mBi_n^-$. *Rapid Commun. Mass Spectrom.* **2009**, *23*, 2663−2668.

(30) Huang, S. Y.; Xie, Z.; Ma, Q. M.; Liu, Y.; Li, Y. C. Geometries, Electronic Structures, and Magnetism of Small Bi_mCo_n Clusters. *J. Mol. Struct.: THEOCHEM* **2010**, *953*, 103−113.

(31) Rangel, E.; Sansores, L. E. Theoretical Study of Neutral Bismuth-Copper, Bismuth-Silver and Bismuth-Gold clusters. *Eur. Phys. J. D* **2013**, *67*, 239.

(32) Martinez, A. Gold−Bismuth Clusters. *J. Phys. Chem. A* **2014**, *118*, 5894−5902.

(33) Kelting, R.; Baldes, A.; Schwarz, U.; Rapps, T.; Schooss, D.; Weis, P.; Neiss, C.; Weigend, F.; Kappes, M. M. Structures of Small Bismuth Cluster Cations. *J. Chem. Phys.* **2012**, *136*, 154309.

(34) Zhai, H. J.; Chen, Q.; Bai, H.; Li, S. D.; Wang, L. S. Boronyl Chemistry: The BO Group as a New Ligand in Gas-Phase Clusters and Synthetic Compounds. *Acc. Chem. Res.* **2014**, *47*, 2435−2445.

(35) Albert, B.; Hillebrecht, H. Boron: Elementary Challenge for Experimenters and Theoreticians. *Angew. Chem., Int. Ed.* **2009**, *48*, 8640−8668.

(36) Sergeeva, A. P.; Popov, I. A.; Piazza, Z. A.; Li, W. L.; Romanescu, C.; Wang, L. S.; Boldyrev, A. I. Understanding Boron through Size-Selected Clusters: Structure, Chemical Bonding, and Fluxionality. *Acc. Chem. Res.* **2014**, *47*, 1349−1358.

(37) Bock, H.; Cederbaum, L.; von Niessen, W.; Paetzold, P.; Rosmus, P.; Solouki, B. Methylboron oxide, $H_3C{-}B{\equiv}O$. *Angew. Chem., Int. Ed. Engl.* **1989**, *28*, 88−90.

(38) Wenthold, P. G.; Kim, J. B.; Jonas, K. L.; Lineberger, W. C. An Experimental and Computational Study of the Electron Affinity of Boron Oxide. *J. Phys. Chem. A* **1997**, *101*, 4472−4474.

(39) Zhai, H. J.; Wang, L. M.; Li, S. D.; Wang, L. S. Vibrationally Resolved Photoelectron Spectroscopy of BO^- and BO_2^-: A Joint Experimental and Theoretical Study. *J. Phys. Chem. A* **2007**, *111*, 1030−1035.

(40) Zubarev, D. Y.; Boldyrev, A. I.; Li, J.; Zhai, H. J.; Wang, L. S. On the Chemical Bonding of Gold in Auro-Boron Oxide Clusters Au_nBO^- (n = 1−3). *J. Phys. Chem. A* **2007**, *111*, 1648−1658.

(41) Zhai, H. J.; Miao, C. Q.; Li, S. D.; Wang, L. S. On the Analogy of B−BO and B−Au Chemical Bonding in $B_{11}O^-$ and $B_{10}Au^-$ Clusters. *J. Phys. Chem. A* **2010**, *114*, 12155−12161.

(42) Bai, H.; Zhai, H. J.; Li, S. D.; Wang, L. S. Photoelectron Spectroscopy of Aromatic Compound Clusters of the B_{12} All-Boron Benzene: $B_{12}Au^-$ and $B_{12}(BO)^-$. *Phys. Chem. Chem. Phys.* **2013**, *15*, 9646−9653.

(43) Chen, Q.; Bai, H.; Zhai, H. J.; Li, S. D.; Wang, L. S. Photoelectron Spectroscopy of Boron-Gold Alloy Clusters and Boron Boronyl Clusters: $B_3Au_n^-$ and $B_3(BO)_n^-$ (n = 1, 2). *J. Chem. Phys.* **2013**, *139*, 044308.

(44) Braunschweig, H.; Radacki, K.; Schneider, A. Oxoboryl Complexes: Boron-Oxygen Triple Bonds Stabilized in the Coordination Sphere of Platinum. *Science* **2010**, *328*, 345−347.

(45) Wang, L. S.; Cheng, H. S.; Fan, J. W. Photoelectron Spectroscopy of Size-Selected Transition Metal Clusters: Fe_n^-, n = 3−24. *J. Chem. Phys.* **1995**, *102*, 9480−9493.

(46) Pyykko, P. Relativistic Effects in Structural Chemistry. *Chem. Rev.* **1988**, *88*, 563−594.

(47) Frisch, M. J.; Trucks, G. W.; Schlegel, H. B.; Scuseria, G. E.; Robb, M. A.; Cheeseman, J. R.; Scalmani, G.; Barone, V.; Mennucci, B.; Petersson, G. A. *Gaussian 09*; Gaussian, Inc.: Wallingford, CT, 2009.

(48) Dennington, R.; Keith, T.; Millam, J. *GaussView*, version 4.1; Semichem, Inc.: Shawnee Mission, KS, 2007.

(49) Suzer, S.; Lee, S. T.; Shirley, D. A. Correlation Satellites in the Atomic Photoelectron Spectra of Group-IIA and -IIB Elements. *Phys. Rev. A: At., Mol., Opt. Phys.* **1976**, *13*, 1842−1847.